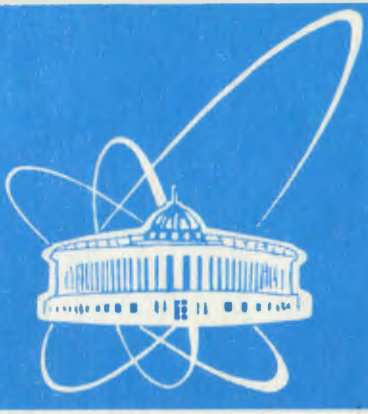

объединенный
институт
ядерных
исследований
дубна

E2-94-348

S.V.Goloskokov[1], O.A.Listopadov[2]

SPIN EFFECTS IN HIGH ENERGY PHOTON-HADRON SCATTERING IN QCD

Submitted to «Ядерная физика»

[1]E-mail address: goloskkv@thsun1.jinr.dubna.su
[2]Scorina University, Gomel, Belarus

1994

At present, the study of spin effects has attracted considerable interest due to the development of polarized programmes at future accelerators [1]. Most part of the spin experimental data at high energies is now obtained at fixed momenta transferred. The t-channel exchange with vacuum quantum numbers (pomeron) gives the main contribution to this region. The vacuum t-channel amplitude is usually associated in QCD with the two-gluon exchange [2]. The spinless pomeron was analysed in [3, 4] on the basis of a nonperturbative QCD model. A similar model was used to investigate the spin effects in the pomeron exchange. It has been shown that different contributions like a gluon [5] and quark loops [6, 7] may lead to the spin-flip amplitude growing as s in the limit $s \to \infty$. As a result, the spin-flip amplitudes are suppressed logarithmically with respect to the spin-non-flip amplitude of the same order in α_s:

$$\frac{|\,T_f\,|}{|\,T_{nf}\,|} \simeq \frac{m\sqrt{|t|}}{a(m,t)\,\ln s}. \qquad (1)$$

Here and in what follows $m = 0.33GeV$ is the constituent quark mass and a is a function linearly dependent on $|t|$ at large $|t|$. The arise of $\ln s$ in (1) stems from the fact that the spin-non-flip amplitude has an additional logarithmical factor. Just this amplitude was calculated in different papers (see [8] e.g.). This result confirms the absence of spin-flip amplitudes in the leading log approximation [9].

In papers [5, 6, 7], the high-energy qq scattering was studied in the soft momentum transfer region $|t| < 1GeV^2$. In [10, 11], spin effects were investigated in the semi-hard region $s \to \infty$, $|t| > 1GeV^2$ where the perturbative theory can be used. Since the spin-flip amplitude growing as s is absent in the born two-gluon diagrams Fig. 1a more complicated ladder diagrams were considered.

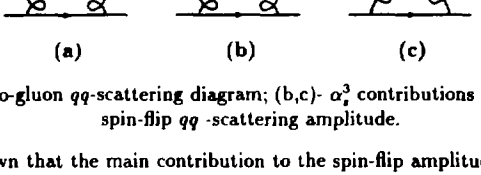

Fig.1 (a)- two-gluon qq-scattering diagram; (b,c)- α_s^3 contributions determining the spin-flip qq -scattering amplitude.

It has been shown that the main contribution to the spin-flip amplitude comes from the planar diagrams of the form, Fig. 1b, 1c. Moreover, there are $s \to u$ crossing diagrams with crossed gluon lines. In the semi-hard region we have $u \simeq -s$ and the real parts are compensated in the sum of diagrams. So we can calculate only the imaginary parts of diagrams in the case of the pomeron exchange. In [10, 11] the factorization spin-flip amplitude T_f into the spin-dependent large-distance part and the high-energy spinless pomeron were shown. This permits one to define the quark-pomeron vertex which is appropriate for the spin-dependent low-energy subgraphs (the upper parts of the graphs

Fig. 1b, 1c) and for investigating the results of summation of the pomeron ladder graphs in higher orders of QCD. As a result of this summation, it has been found that the ratio $T_{flip}/T_{non-flip}$ is energy-independent. The obtained total spin flip amplitude [10, 11] is about 2 per cent of the spin-non-flip one. Note that the smallness of the resulting spin-flip amplitude is caused by the compensation of different matrix structure contributions, that are not very small by themselves. Compensation like that is possible only for the quarks *on the mass shell. Really, the model investigations of the* γq *elastic scattering at high* energies [10, 7] show that the off-mass-shell effects in the quark loop increase the spin-flip amplitude essentially.

The purpose of this paper is to investigate the role of the off-mass-shell effects of the wave functions in the semi-hard region. The role of these effects is studied by using the elastic γq- scattering as an example. The contributions from the hadron wavefunction are very similar to the quark-loop integral in this reaction and all calculations can be performed up to the end without taking any additional information about the hadron spin structure into account. Moreover, the investigation of γq-scattering is of major methodical importance since it is the simplest subprocess in photon-hadron reactions. For example, the reactions of diffractive photoproduction of vector mesons differ from the above only by the replacement of the wavefunction of the outgoing photon by the meson wavefunction.

Let us investigate the elastic γq-scattering

$$\gamma\,(p_1)\;+\;q\,(p_2)\;=\;\gamma\,(p_3)\;+\;q\,(p_4).$$

In what follows, we shall use the symmetric coordinate system in which the sum of quark momenta before and after scattering is directed along the z-axis:

$$q=\frac{p_1+p_3}{2}=(p_0,0,0,p_z),\qquad p'=\frac{p_2+p_4}{2}=(p_0,0,0,-p_z), \tag{2}$$

and the momenta transferred Δ, along the x-axis [5]:

$$r=\frac{p_1-p_3}{2}=\frac{p_2-p_4}{2}=(0,-\Delta/2,0,0). \tag{3}$$

In the present paper only the planar graphs (which contain an interaction of the gluons from the pomeron with one quark in the loop) will be considered since just they determine effects under study. The main contribution to the elastic γq-scattering amplitude in the semi-hard region in the α_s^2 order comes from the imaginary part of the diagram drawn in Fig. 2a. In calculations, we shall use the Feynman gauge because only the $g_{\mu,\nu}$ terms in the t-channel gluon propagators contribute to the leading $\sim s$ terms of the scattering amplitudes, and in the α_s^3 order we do not have ghost contributions.

Let us calculate the matrix element of the amplitude, Fig. 2a, with spin-flip and spin-non-flip of the photon. As has been shown in [5], the main contribution to the amplitude is determined by the following spin-non-flip matrix element structure in the lower quark line

$$\bar{u}^+(p'+r)\gamma^\nu(\hat{p}'+\hat{l}+m)\gamma^\nu u^+(p'-r)\simeq 4p'^\mu p'^\nu. \tag{4}$$

Then, the matrix element of the amplitude can be written as follows:

$$M=N^{\mu,\nu}4p'_\mu p'_\nu, \tag{5}$$

where $N_i^{\mu\nu}$ is a matrix structure of the upper graph's part.

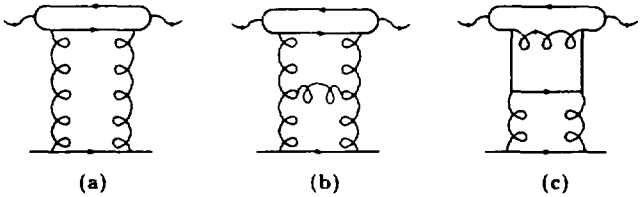

(a) (b) (c)

Fig.2 The planar contributions to the γq -scattering amplitude (a)- born diagram; (b,c)- α_s^3 contributions.

Now let us calculate the imaginary parts of the spin-non-flip matrix elements in the down quark line $\langle T^i_{Born}(s,t)\rangle$ of diagram Fig. 2a. They have the form

$$\mathrm{Im}\langle T^i_{Born}(s,t)\rangle = cof \int d^4p d^4l \delta[(p-q)^2 - m^2]\delta[(p-l)^2 - m^2]$$

$$\delta[(p'+l)^2 \quad m^2]\left[M^i_{Born}\right] \prod(G(p\pm r)) \prod(F(l\pm r)), \tag{6}$$

where cof is a numerical factor, $G(p\pm r)$ is the quark propagator functions from the upper part of the graph, $F(l\pm r)$ are the gluon propagators from the lower part of the graph, M^i_{Born} include the corresponding matrix elements of the diagram's numerator. It is useful to perform calculations in the light-cone variables

$$p = (zq_+, p_-, p_\perp),\ k = (xq_+, k_-, k_\perp),\ l = (yq_+, l_-, l_\perp),\ q_\pm = q_0 \pm q_z\ . \tag{7}$$

After integration with the δ-functions, we obtain the following representation:

$$\mathrm{Im}\langle T^i_{Born}(s,t)\rangle = cof \frac{1}{s}\int_{sc/s}^{1} \frac{dz}{z(1-z)} \int d^2p_\perp d^2l_\perp$$

$$\left[M^i_{Born} \prod(G(p\pm r)) \prod(F(l\pm r))\right]\Big|_{(q_+p_-),(q_+l_-),y}. \tag{8}$$

Here $(q_+p_-),(q_+l_-),y$ are pole solutions of the δ-functions, the numerical factor has the form:

$$cof = 4\pi\,\alpha_s^2\,\alpha,\ \frac{(-1)}{16\pi^2}c_2,\ \ c_2 = \frac{8}{36}\ . \tag{9}$$

c_2 is a color factor of the born two-gluon diagram (Fig. 1a). For the diagram investigated the functions G and F look as follows:

$$G(p\pm r) = -\frac{1-z}{m^2 + [p_\perp \pm r_\perp(1-z)]^2}, \tag{10}$$

$$F(l\pm r) = -\frac{1}{\lambda^2 + [l_\perp \pm r_\perp]^2}, \tag{11}$$

where we introduce the mass λ in the gluon propagators. The matrix elements of the diagram have the following form:

$$M^{flip}_{Born} = 8s^2\Delta^2 z^2(z-1)^2 \tag{12}$$

$$M_{Born}^{non-flip} = \frac{4s^2}{1-z}\left[(2z^4 - 6z^3 - 7z^2 - 1z + 11)\Delta^2 - 4m^2\right]. \qquad (13)$$

This means that the spin-flip and spin-non-flip matrix elements are growing as s^2. One power of s is compensated in the integral (8) and both the spin flip and non-flip amplitudes are growing as s; that is taking the off-mass-shell effects into account leads to the energy-independent ratio of spin-flip and spin-non-flip amplitudes in the same α_s order.

The born two-gluon high-energy amplitude (Fig. 1a) has the form [10, 11]:

$$\hat{T}^{2g}(s,t) = A^{2g}(s,t)\frac{\hat{p}'}{s}, \qquad (14)$$

where

$$A^{2g}(s,t) = 4is\alpha_s^2 c_2 \int d^2l_\perp \prod (F(l \pm r)), \quad c_2 = \frac{8}{36}, \qquad (15)$$

with $(F(l \pm r))$ determined in (11).

Note that the contribution of the radiative corrections in (14) can be taken into account through the use of the spinless pomeron vertex function (formfactor)

$$\frac{\mu_0^2}{\mu_0^2 + \Delta^2}, \quad \mu_0 \sim 1\,GeV, \qquad (16)$$

which was introduced in [4]. It is easy to see that the integrals over $d^4p_\perp$ and $d^2l_\perp$ are factorized completely in (8). Moreover, the integrals over $d^2l_\perp$ coincide with the transverse integral in (15). So, expression (8) may be written in the form:

$$\mathrm{Im}(T^1_{Born}(s,t)) = \alpha_s A^{2g}(s,t)\ \Phi^{\gamma q}_{Born}, \qquad (17)$$

where

$$\Phi^{\gamma q}_{Born} = \frac{(-1)}{4\pi^2}\int_{z_0/s}^{1}\frac{dz\ [M^1_{Born}]}{s^2\, z(1-z)}\int d^2p_\perp \prod (G(p \pm r)). \qquad (18)$$

The obtained result (17) confirm the factorization in the spin-flip part of the pomeron exchange of the large-distance effects $\Phi^{\gamma q}_{Born}$ and the high energy spinless two gluon amplitude $A^{2g}(s,t)$.

The main contribution to the γq-scattering amplitude in the α_s^3 order comes from the imaginary part of the diagrams drawn in Figs. 2b, 2c. We will also take into account the α_s^3 order contributions to the spin-non-flip amplitude in contrast with [10, 11]. As it will be shown, the cross-section's shape depends essentially on these contributions. Let us calculate the imaginary parts of the spin-non-flip matrix elements in the down quark line $\langle T^1_{a,b}(s,t)\rangle$ of the diagrams Fig. 2b, 2c. After integration with the δ-functions in the light-cone variables (7) we obtain the following representation similar to (8):

$$\mathrm{Im}(T^1_{1,2}(s,t)\rangle = cof_{1,2}\frac{1}{s}\int_{z_0/s}^{1}\int_{z_0/z}^{z}\frac{dz\,dx}{(1-z)(z-x)x}\int d^2p_\perp d^2k_\perp d^2l_\perp$$

$$\left[M^1_{1,2}\prod(G(p \pm r))\prod(G_{1,2}(k \pm r))\prod(F(l \pm r))\right]\Big|_{(q_+p_-),(q_+k_-),(q_+l_-),0}. \qquad (19)$$

Indices "1", "2" denote that the quantity refers to graph Fig. 2b or 2c, respectively. The numerical factors (c_2 was determined in (9)) have the form:

$$cof_1 = 4i\,\alpha_s^2\,\alpha_r\,\frac{1}{(2\pi)^4}\,3c_2, \tag{20}$$

$$cof_2 = 4i\,\alpha_s^2\,\alpha_r\,\frac{1}{(2\pi)^4}\,\frac{4}{3}c_2. \tag{21}$$

For the diagrams investigated the functions G and F look as follows:

$$G(p \pm r) = -\frac{1-z}{m^2 + [p_\perp \pm r_\perp(1-z)]^2}, \tag{22}$$

$$F(l \pm r) = -\frac{1}{\lambda^2 + [l_\perp \pm r_\perp]^2}, \tag{23}$$

$$G_{1,2}(k \pm r) = -\frac{z-x}{z\left[a_{1,2} + (k_\perp \pm r_\perp b)^2\right]},$$

$$b = \frac{z-x}{z}, \quad a_1 = \frac{m^2 x(1-x)}{z(1-z)} + \frac{\lambda^2(z-x)}{z} + \frac{x(z-x)(1-z)r_\perp^2}{z^2}, \tag{24}$$

$$a_2 = \frac{m^2 x(z-x)(x-z+1)}{z(1-z)} + \frac{\lambda^2 x}{z} + \frac{x(z-x)(1-z)r_\perp^2}{z^2}.$$

It follows from (22), (23), (24) that in the $\lambda \to 0$ limit we have infrared singularities only from the gluon propagators $F(l \pm r)$ in the down part of the graph. All other propagators do not have divergences in this limit.

The matrix elements of the diagrams have the following form:

$$M_1^{flip} = 4s^2\Delta^2 m^2 x\left[8x^2z - 12x^2 + 2xz^2 - 8xz + 5x + 5z\right], \tag{25}$$

$$M_1^{non-flip} = \frac{4s^2\Delta^2 m^2 x}{z(1-z)}$$

$$\Big[8x^2z^3 - 20x^2z^2 + 16x^2z - 4x^2 + 2xz^4 - \tag{26}$$

$$10xz^3 + 19xz^2 - 16xz + 5z^3 - 10z^2 + 10z\Big],$$

$$M_2^{flip} = -16s^2\Delta^2 m^2 x^2\left[2xz - 3x - 4z^2 + 8z - 1\right], \tag{27}$$

$$M_2^{non-flip} = \frac{16s^2\Delta^2 m^2 x^2}{z(z-1)} \tag{28}$$

$$\left[2xz^3 - 5xz^2 + 4xz - x - 4z^4 + 12z^3 - 13z^2 + 6z\right].$$

Hence, the spin-flip matrix elements and the spin-non-flip one of the ladder diagrams are growing as s^2 as well. One power of s is compensated in the integral (19) and both the spin-flip and non-flip amplitudes are growing as s. The ratio of spin-flip and spin-non-flip

amplitudes is independent of the energy in the α_s^3 order in the same manner as for α_s^2. As one can see, the integrals over $d^2p_\perp$, $d^2k_\perp$ and $d^2l_\perp$ are factorized completely in (19). Using (15) as notation, the amplitudes (19) can be written in the form:

$$\mathrm{Im}\langle T^i_{1,2}(s,t)\rangle = \alpha_s A^{2g}(s,t)\ \Phi^{\gamma q}_{1,2}, \tag{29}$$

where

$$\Phi^{\gamma q}_{1,2} = \frac{\alpha_s}{(2\pi)^4} C_{1,2} \int_{s_0/s}^{1} \int_{s_0/s}^{z} \frac{dz\,dx}{s^2\,(1-z)(z-x)\,x} \left[M^i_{1,2} \right]$$
$$\int d^2p_\perp \prod (G(p \pm r)) \int d^2k_\perp \prod (G_{1,2}(k \pm r)) \tag{30}$$

$$C_1 = 3, \quad C_2 = \frac{4}{3}.$$

We have obtained again the factorization (29) in the spin-flip part of the pomeron exchange of the large-distance effects $\Phi^{\gamma q}_{1,2}$ and the high energy spinless two gluon amplitude $A^{2g}(s,t)$.

In calculation, we use $\alpha_s = 0.3$ which is typical of $|t| \sim 1 GeV^2$ and $\lambda = 0.1 GeV$.

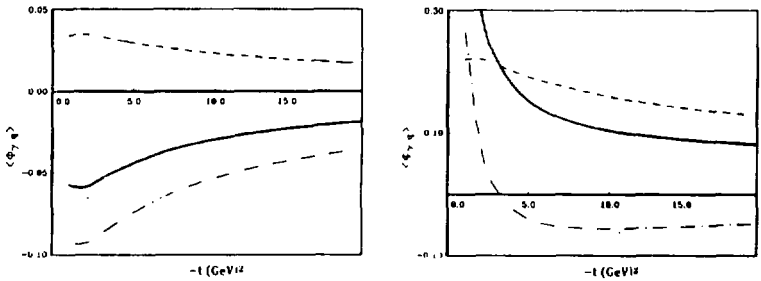

(a) (b)

Fig.3 Different contributions to the $\Phi^{\gamma q}$ spin-flip amplitude -(a) and spin-non-flip amplitude- (b): dot-dashed curves for the born (Fig. 2a) diagram with the formfactor are taken into account; dashed curves for the ladder (Fig. 2b,c) diagrams; full line for the total amplitude.

The obtained results are shown in Fig. 3 and 4, where the $|t|$-dependence of the amplitudes $\Phi^{\gamma q}$ is displayed. In Fig. 3, the contribution of the born diagram subject to the formfactor (see (16)) is presented. In Fig. 4, this contribution is shown without considering the formfactor. It is easy to see that the cross-section's shape essentially depends on the consideration of the formfactor and the contributions in the α_s^3 order to the spin-non-flip amplitude. Actually, the total non-flip amplitude in Fig. 3 does not have a dip in contrast with the one in Fig. 4. This fact means, respectively, the lack or the availability of diffractive minimum in the cross-section. Hence, the obtained result

may help to refine the formfactor expression (16) from the experimental data on the cross-section.

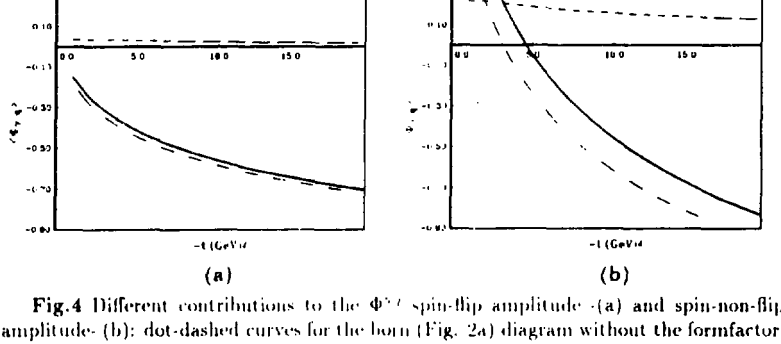

Fig.4 Different contributions to the Φ^0 spin-flip amplitude (a) and spin-non-flip amplitude (b): dot-dashed curves for the born (Fig. 2a) diagram without the formfactor; dashed curves for the ladder (Fig. 2b,c) diagrams; full line for the total amplitude.

Let us consider the conclusions which may be drawn from the performed calculation. As have been noted above, the spin-flip amplitudes are suppressed logarithmically with respect to the spin-non-flip one for the quarks on the mass shell and for the diagrams in the same α_s order. As has been shown, the taking off-mass-shell effects of the wave function into account leads to the energy-independence of the ratio $T_{flip}/T_{non-flip}$ in α_s^2 and α_s^3 order. One would expect that in higher α_s orders the energy-independence of this function holds true. The next conclusion implies that the wave function has no effect on the factorization of the large-distance contributions and the high energy spinless two-gluon amplitude in T_{flip}. The most important conclusion to emerge from the obtained results is that the spin-flip amplitude is not small with respect to the spin-non-flip one. Its magnitude may run to 20-30% of the spin non-flip amplitude. It should be emphasized that the obtained here spin-flip amplitudes are completely determined by low-energy effects in the quark (gluon) loop. Hence, the performed calculation shows that off-mass-shell effects in the quark-loop essentially increase the contributions of the spin-dependent quark-pomeron vertex to the amplitude with photon's spin-flip. Such spin effects may lead to considerable spin asymmetries in the reactions of the vector meson production which will be studied at future accelerators. Note that it is necessary to find a relative phase between spin-flip and non-flip amplitudes for the spin asymmetry computing. These calculations and investigation of the diffractive photoproduction of vector meson reactions will be performed later.

Acknowledgement. The authors express their deep gratitude to V.A.Meshcheryakov and A.N.Sissakian for the support in this work and to A.V.Efremov, W.D.Nowak and O.V.Teryaev for fruitful discussions. O.L. would also like to thank V.G.Teplyakov.

This work was supported in part by the Russian Fond of Fundamental Research, Grant 94 – 02 – 04616.

References

[1] G.Bunce et al., Particle World, 1992, V.3, P.1.

[2] F.E.Low, Phys.Rev., 1975, V.D12, P.163.
S.Nussinov, Phys.Rev.Lett., 1975, V.34, P.1286.

[3] P.V.Landshoff, O.Nachtmann, Z.Phys.C Particles and Fields, 1987, V.35, P.405.

[4] A.Donnachie, P.V.Landshoff, Nucl.Phys., 1989, V.B311, P.509.

[5] S.V.Goloskokov, Yad.Fis., 1989, V.49, P.1427.

[6] S.V.Goloskokov, Yad.Fis., 1990, V.52, P.216.

[7] S.V.Goloskokov, J.Phys. G:Nucl.Part.Phys., 1993, V.19, P.67.

[8] B.M.McCoy, T.T.Wu, Phys.Rev., 1975, V.D12, P.3257.
H.T.Nich, Y.P.Yao, Phys.Rev., 1976, V.D13, P.1082.
L.Tybursky, Phys.Rev., 1976, V.D13, P.1107.

[9] E.A.Kuraev, L.N.Lipatov, S.V.Fadin, Zh.Eksp.Teor.Fiz., 1977, V.72, P.377.

[10] S.V.Goloskokov, Phys.Lett., 1993, V.B315, P.159.

[11] S.V.Goloskokov, O.V.Selyugin, Yad.Fis., 1994, V.57, P.727.

[12] S.J.Brodsky et al., Preprint SLAC-PUB-6412, 1994.

Received by Publishing Department
on August 30, 1994.